

# Intermetallic compound formation between Sn–3.5Ag solder and Ni-based metallization during liquid state reaction

Min He<sup>a</sup>, Wee Hua Lau<sup>a</sup>, Guojun Qi<sup>b</sup>, Zhong Chen<sup>a,\*</sup>

<sup>a</sup>*School of Materials Engineering, Nanyang Technological University, Nanyang Avenue, Singapore 639798, Singapore*

<sup>b</sup>*Singapore Institute of Manufacturing Technology, 71 Nanyang Drive, Singapore 638075, Singapore*

Available online 24 June 2004

## Abstract

Ni and its alloys possess a lower reaction rate with Sn than Cu and Cu alloys. Ni-based under bump metallization (UBM) therefore receives considerable attention from the microelectronic packaging industry for the popular flipchip applications. In this work, we study the interfacial reaction of electroless Ni–P (EN) alloy and Ni UBMs with Sn–3.5Ag solder. Morphology and growth kinetics of the formed Ni<sub>3</sub>Sn<sub>4</sub> intermetallic compound (IMC) in both systems are investigated under different reflow durations. With the Ni–P alloy as the UBM, needle-type, boomerang-type and chunk-type IMC grains coexist at short reflow time, but only chunk-type grains remain after prolonged reflow. With pure Ni as UBM, only scallop grains with faceted surfaces are found under both short and long reflow durations. The thickness of the intermetallic compound in both UBM systems is measured under different reflow conditions, from which the growth kinetics parameters are obtained. It is found that the IMC growth rate is higher with the Ni–P UBM than with pure Ni UBM. Another difference between the two UBMs is the existence of Kirkendall voids at the interface: the voids are found inside the Ni<sub>3</sub>P layer in the Ni–P UBM system after long-time reflow. However, such voids are not observed in the pure Ni UBM system.

© 2004 Elsevier B.V. All rights reserved.

**Keywords:** Lead-free solder; Under bump metallization; Intermetallic compound; Kirkendall voids

## 1. Introduction

All these years, a eutectic Sn–Pb solder has been the first choice in the electronic industry. This is primarily due to the combined merits of low cost, good soldering properties, adequate melting temperature range and proper physical, mechanical, metallurgical and fatigue properties. Due to concerns about the environmental pollution of lead, lead-free solders (most of them contain more than 90 wt.% Sn) are becoming popular [1–5]. However, many technical issues arise from the conversion to lead-free solder applications. A typical problem encountered is that these Sn-based lead-free solders were found incompatible with traditional Cu-based metallizations due to rapid reaction and spalling of Cu–Sn intermetallic compounds (IMCs) [6–8]. As alternatives, nickel-based under bump metallizations (UBMs), such as electroless Ni–P (EN) alloys and pure

Ni, have attracted attention in recent years because of their good wettability [9] and slow reaction rate with solders [6,10].

The interfacial reaction between Ni-based UBM and solders, either eutectic Sn–Pb or lead-free, has been a topic of many studies [6,8,10–15]. Most of the studies were conducted for relatively short times for liquid state solder reaction. The time corresponds well to the time employed in the packaging industry. In this work, however, we studied the interaction of molten Sn–3.5Ag solder with two types of Ni-based UBMs (electroless Ni–P and pure Ni) for reflows ranging from the conventional short time to an extended long time. The purpose is to establish a comprehensive database for the liquid state reactions between Sn–3.5Ag solder and the two types of UBMs. The thickness of the common IMC, Ni<sub>3</sub>Sn<sub>4</sub>, in both systems was measured under different reflow parameters and its growth kinetics parameters were calculated. Attention was paid to the Kirkendall voids formation during reflow and comparison was made, whenever possible, on the difference between the two UBM systems.

\* Corresponding author. Tel.: +65-67904256; fax: +65-67909081.  
E-mail address: [aszchen@ntu.edu.sg](mailto:aszchen@ntu.edu.sg) (Z. Chen).

## 2. Experimental procedures

The substrates used in this study were prepared from blank Si wafers. Pure nickel UBM was prepared by sputtering the deposition of about 0.1- $\mu\text{m}$ -thick chromium first, followed by about 1- $\mu\text{m}$  nickel and 0.3- $\mu\text{m}$  gold. The chromium layer provides good adhesion of the UBM to the wafer. For the preparation of the Ni–P UBM, sputtered pure nickel was used as the seed layer for the subsequent electroless plating of Ni–P alloy. In current work, Ni–P (12.5 at.% P) UBM of about 5  $\mu\text{m}$  in thickness was obtained with a commercial electroless nickel solution. Before the plating, the sputtered 0.3- $\mu\text{m}$  gold layer was etched away. A final finish by immersion gold (about 0.05- $\mu\text{m}$  thick) on the plated Ni–P was applied as a surface protection.

Sn–3.5Ag solder was in the form of wire with no-clean reflow flux in the core. The solder wire was cut and placed in contact with the UBM. The samples of both Ni-based UBMs were reflowed in the oven for different holding times from 5 s to 5 h at 251  $^{\circ}\text{C}$ . They were then taken out of the oven and cooled in air.

Reflowed samples were prepared for observations on the cross section as well as from the top of the intermetallic compounds (IMC) at the solder/UBM interface. The common metallography practice was used to prepare the samples. An etchant of 2% HCl was used to reveal the cross-sectional microstructure. In order to observe the top view of the IMCs, majority of the solder on the specimens was first ground away. The ground specimens were then etched with 2% HCl to dissolve the remaining solder. The average thickness of the IMC was obtained by measuring the cross-sectional area of the IMC layer over a certain length from SEM images.

## 3. Results and discussion

### 3.1. Intermetallic compound formation

#### 3.1.1. Intermetallics formed during reflow

Figs. 1 and 2 are respective SEM micrographs of the interfacial microstructure of Sn–3.5Ag solder with the Ni–P and pure Ni UBMs reflowed at 251  $^{\circ}\text{C}$  for different holding times. The IMC layer structure was observed at the solder/UBM interfaces in the cross-sectional view. For Ni–P UBM, a layer of mainly  $\text{Ni}_3\text{P}$  crystals (referred to as  $\text{Ni}_3\text{P}$  in the following text) is sandwiched in between  $\text{Ni}_3\text{Sn}_4$  and the UBM. For the Ni UBM, only  $\text{Ni}_3\text{Sn}_4$  IMC forms between the solder and the unconsumed Ni UBM. Au dissolves readily into the molten solder soon after reflow begins, no Au intermetallic compound was detected at the interface. These observations of the main interfacial reaction products are in agreement with what were reported by other researchers [14–17]. By employing the same reflow condition, this study finds that the interface between IMC and the UBM is flatter with Ni UBM than with Ni–P UBM

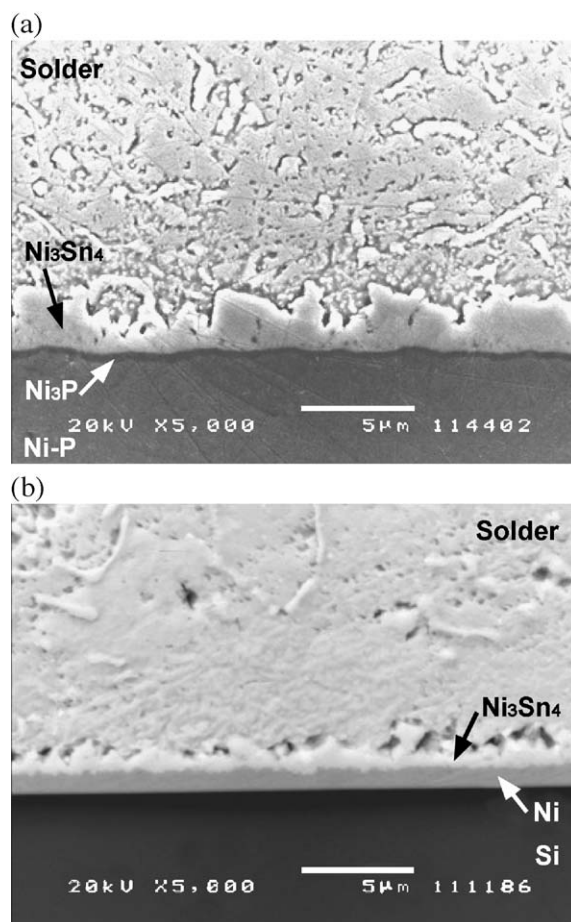


Fig. 1. Sn–3.5Ag solder with Ni-based UBMs reflowed for 180 s at 251  $^{\circ}\text{C}$ . (a) Electroless Ni–P UBM. (b) Sputtered Ni UBM.

(compare Figs. 1a,b and 2a,b). In both cases, the thickness of the Ni–Sn IMC increases with reflow time at the expense of UBM thickness. However, the  $\text{Ni}_3\text{Sn}_4$  IMC layer formed with sputtered Ni UBM is thinner than that with the Ni–P UBM system under the same reflow condition.

Phosphorus was not detected in the IMC phase. Nevertheless, this study finds that it plays an important role in the interfacial reaction. From the cross-sectional SEM micrographs, a notable difference between two UBMs is the formation of the crystalline  $\text{Ni}_3\text{P}$  phase with Ni–P UBM. The  $\text{Ni}_3\text{P}$  forms as a result of Ni depletion from the UBM to form  $\text{Ni}_3\text{Sn}_4$ , which has facilitated the crystallization of the amorphous Ni–P [7]. In the case of Ni UBM, only  $\text{Ni}_3\text{Sn}_4$  IMC is formed by direct consumption of nickel. According to Liu and Shang [12],  $\text{Ni}_3\text{P}$  has a crystal structure with very fine grains. These fine grains influence the diffusion of Ni through this layer. Relatively faster diffusion of nickel at certain locations results in the different shape and thickness of  $\text{Ni}_3\text{Sn}_4$  IMC grains along the interface.

#### 3.1.2. Morphology of the $\text{Ni}_3\text{Sn}_4$ intermetallic compound

The top views of the IMC morphologies for the two types of solder/UBM joints are shown in Figs. 3–5 for samples

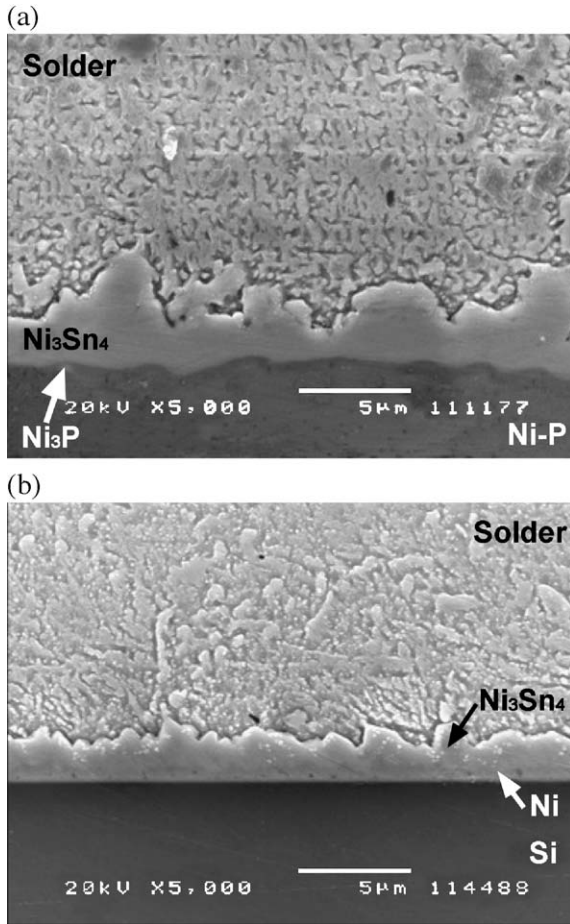


Fig. 2. Sn–3.5Ag solder with Ni-based UBMs reflowed for 600 s at 251 °C. (a) Electroless Ni–P UBM. (b) Sputtered Ni UBM.

reflowed at 251 °C for different durations. After reflow for only 5 s in Sn–3.5Ag on Ni–P UBM, a very thin layer of IMC, which consists of fine needles as shown in Fig. 3(b), has been formed with some boomerang-like large grains. A large space exists in between these needle-like IMC grains. When reflow time extended to 30 s, needle-like IMC grains remain dominant, but the number of boomerang-type and chunk-type grains increases as shown in Fig. 4(a). When reflow time reaches 90 s, majority of the IMC grains becomes boomerang-type and chunk-type, as shown in Fig. 4(b). Grain sizes of both boomerang-type and chunk-type grains increase with reflow time. After 180 s of reflow at 251 °C, the  $\text{Ni}_3\text{Sn}_4$  IMCs formed in electroless Ni–P UBM system display a variety of grain sizes and shapes, as shown in Fig. 4(c): chunk-type, boomerang-type and needle-type  $\text{Ni}_3\text{Sn}_4$  IMC grains are all present. When reflow time extends to 600 s, all IMC grains become chunk-type, as illustrated in Fig. 4(d). With the extension of liquid state reaction time, the small needle-type and boomerang-type grains either grow to larger sizes or disappear because of ripening reaction.

The IMCs formed on Ni UBM, on the other hand, are all scallop-type grains with faceted surfaces as shown in

Fig. 5. Their size grows with time but there is no shape change as in the case of Ni–P UBM. By comparing with the results obtained from the Sn–3.5Ag/Ni–P combination, it is clear that the existence of P in the UBM affects the  $\text{Ni}_3\text{Sn}_4$  morphology. In fact, it affects not only the IMC morphology but also IMC growth speed as will be discussed later.

### 3.1.3. IMC grain coarsening and formation of extremely large $\text{Ni}_3\text{Sn}_4$ grains

Intermetallic grain size continues to increase and the total number of grains decreases during liquid solder/UBM interaction. Kim and Tu [18] suggested that this type of nonconservative grain coarsening was controlled by two fluxes—diffusion flux from UBM to interface and ripening flux due to curvature of grains [18]. Based on their scallop grain model with a narrow channel between scallops, which is commonly seen in Cu–Sn system, the  $t^{1/3}$  growth behavior was proposed. Ghosh [11] studied various types of Sn-based solders with Ni UBM for up to 600 s of reflow. The work supported Kim and Tu's [18] model stating that

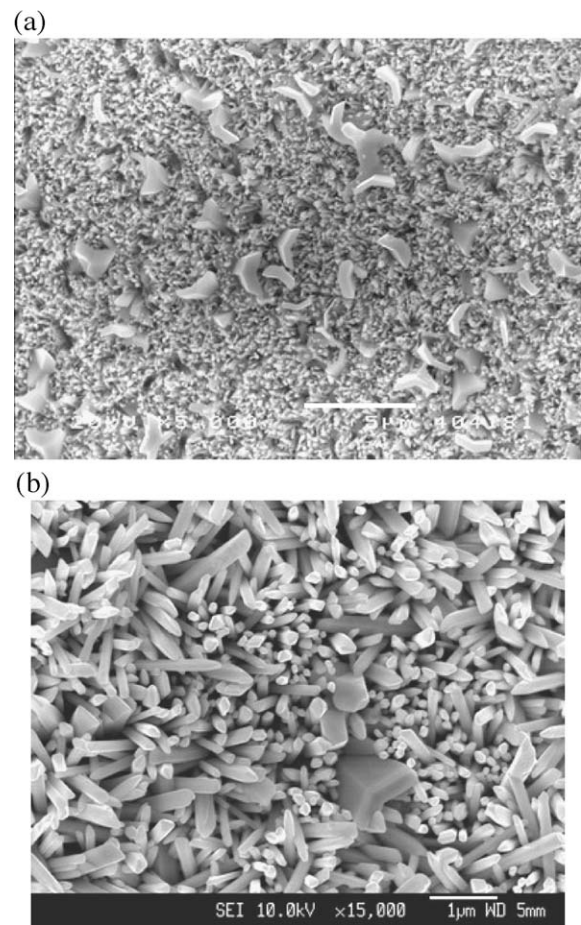


Fig. 3. (a)  $\text{Ni}_3\text{Sn}_4$  IMC in a Ni–P UBM system reflowed at 251 °C for 5 s. (b) Magnified picture of (a) showing that plenty of space exists between the IMCs.

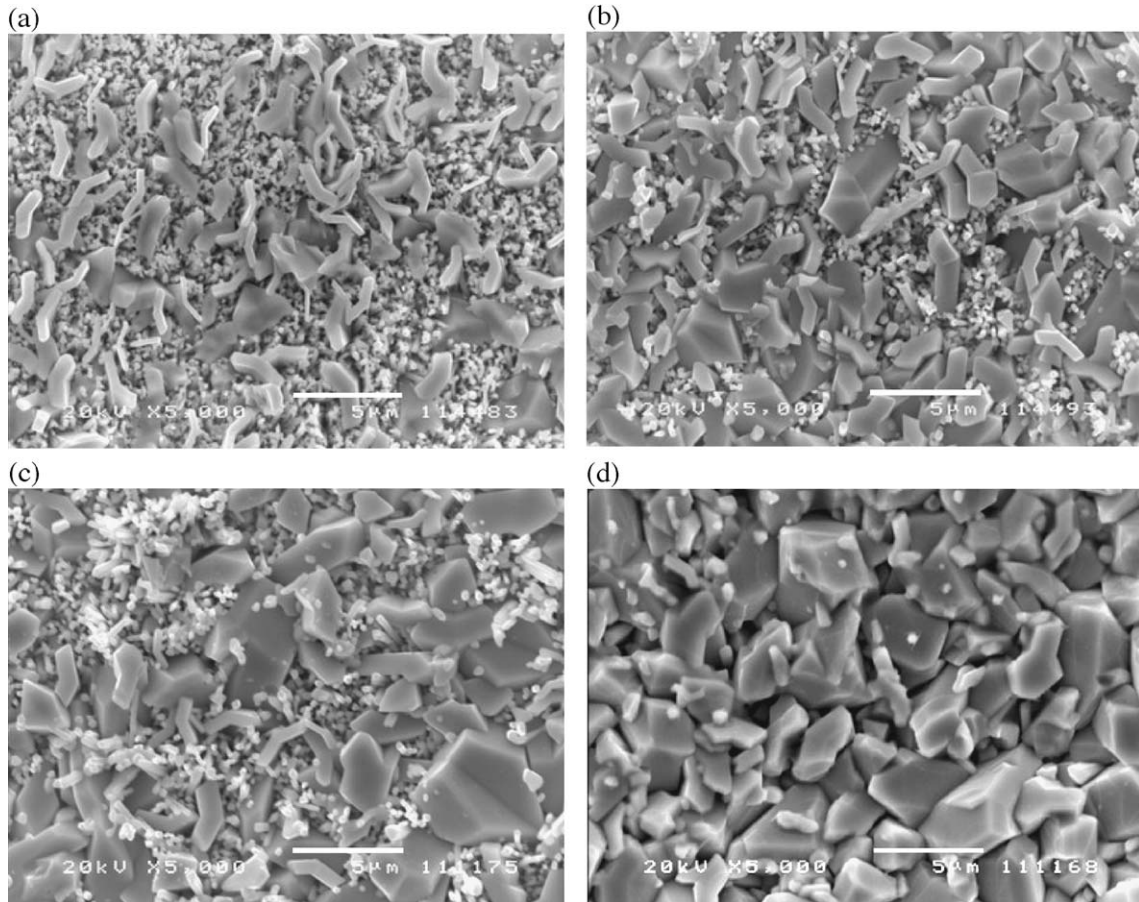


Fig. 4.  $\text{Ni}_3\text{Sn}_4$  IMC in a Ni–P UBM system after different reflow time at 251 °C: (a) 30 s; (b) 90 s; (c) 180 s; and (d) 600 s.

the diffusion of Ni through the narrow channels between  $\text{Ni}_3\text{Sn}_4$  grains might be the rate-controlling step for the growth of  $\text{Ni}_3\text{Sn}_4$ . However, the power law constants from Ghosh's [11] experiment were generally less than 1/3. Other factors such as IMC grain faceting and coalescence were cited to be accountable for the discrepancy [11].

The observation of IMC growth in our work generally follows the predicted trend of grain coarsening. After its formation, the IMC grain coarsens and facets continuously in a prolonged reflow process. The facet is due to the anisotropic interfacial energy of the  $\text{Ni}_3\text{Sn}_4$  phase. What has not been reported before is the formation of extremely large IMC grains after 20 min of reflow in both solder/Ni-based UBM systems, as shown in Figs. 6 and 7. We speculate that the large grains form when a number of neighboring IMC grains happen to possess the same crystallographic orientation; these grains can easily coalesce to form a large grain. At extended reflow time when the IMCs form a continuous layer, the diffusion flux from UBM becomes weaker than that at the initial stage when liquid solder is in direct contact with the UBM through the grooves between IMCs. As a result, ripening becomes the controlling flux for grain growth at extended reflow time. Existing large grains grow at the expense of smaller ones under ripening flux.

#### 3.1.4. Spallation of intermetallics

The interfacial intermetallic compounds may spall into the molten solder for two reasons. During IMC formation, there inevitably exist mechanical stresses due to the volume difference between the reaction metallization and the formed IMC. The other reason is the wettability of the IMC to the underlying layer.

When all the sputtered 1- $\mu\text{m}$  Ni UBM has been consumed after around 40 min of reflow, spallation and delamination of some  $\text{Ni}_3\text{Sn}_4$  grains can be observed, as shown in Fig. 8. The delamination indicates that  $\text{Ni}_3\text{Sn}_4$  does not wet the underlying Cr layer well. In order to verify that complete consumption of Ni is indeed the cause for the delamination, an additional experiment was carried out using a much thicker (250  $\mu\text{m}$ , 99.98% purity) Ni foil as UBM. In this case, Ni was not be used up for an extremely long reflow. It was found that some IMCs spalled into the molten solder, but there was always a layer of IMC that attached to the Ni UBM. Fig. 9 shows the result after 18 h of reflow with the thick Ni UBM. The same micrograph also showed a segment of the interface covered by extremely large IMC grains. Comparing the results of both thin and thick Ni UBMs, current work suggests that the stress, which will be discussed in detail later, causes the IMC spallation on Ni UBM. The wettability of the IMC on the Ni-based UBM is

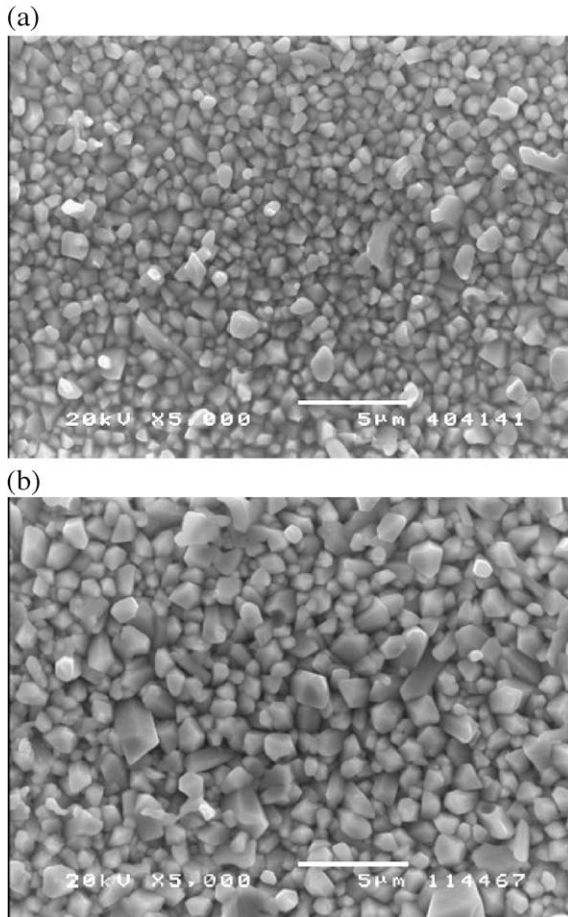


Fig. 5.  $\text{Ni}_3\text{Sn}_4$  IMC in a sputtered Ni UBM system after different reflow time points at 251 °C: (a) 180 s and (b) 600 s.

strong enough to prevent its delamination. The detachment of IMC from the substrate only occurs when Ni is fully consumed, which indicates a poor adhesion between  $\text{Ni}_3\text{Sn}_4$  and Cr.

In the Ni–P UBM system, spallation of  $\text{Ni}_3\text{Sn}_4$  IMC was not observed even after reflow for 5 h at 251 °C. In a study

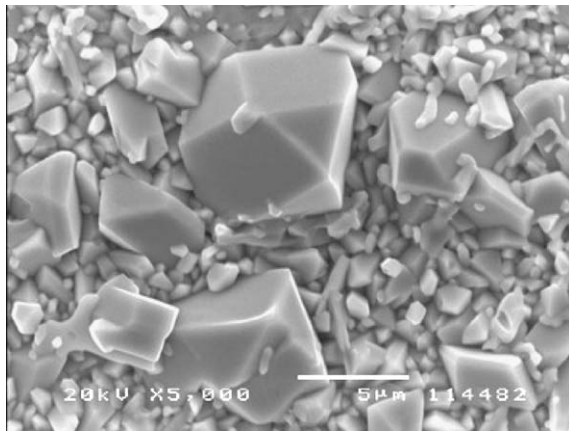


Fig. 6. Extremely large  $\text{Ni}_3\text{Sn}_4$  grains in a Sn–3.5Ag/sputtered Ni UBM system reflowed for 20 min at 251 °C.

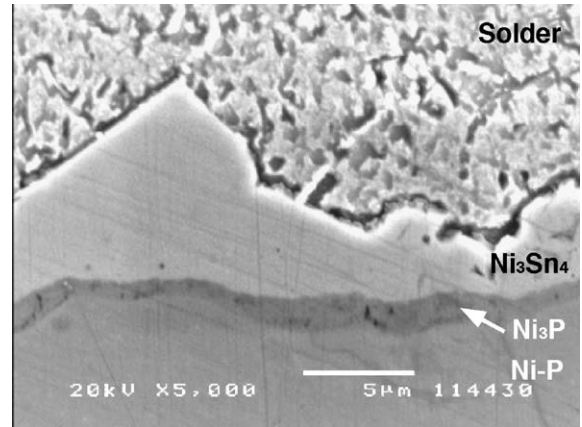


Fig. 7. Cross-sectional view of extremely large  $\text{Ni}_3\text{Sn}_4$  grains formed in a Sn–3.5Ag/Ni–P system after being reflowed for 1 h.

conducted by Hung et al. [13] on eutectic SnPb solder with Ni–P UBM, spallation was also not observed for up to 90 min of reaction. The reason for the difference with Ni UBM could be due to the nature of the stress generated at the interface. The density of the Ni–P alloy containing 12.5 at.% P is around 8.0 g/cm<sup>3</sup>, while the densities of pure Ni and  $\text{Ni}_3\text{Sn}_4$  IMC are 8.9 g/cm<sup>3</sup> and 8.64 g/cm<sup>3</sup>, respectively. Although it is difficult to estimate the magnitude of the stress during the formation of IMC through this liquid–solid reaction, it is reasonable to suggest that the nature of stress is compressive when the IMC is formed on pure Ni UBM. As the IMC layer becomes thick, the compressive stress tends to squeeze out the IMCs causing the spallation. In the case of Ni–P UBM, the stress is tensile in the IMC layer. A tensile stress, once built up sufficiently, may cause fracture of a continuous layer but not spallation. In fact, the IMC layer is not really continuous at the early stage of reflow because there are many grooves between neighboring

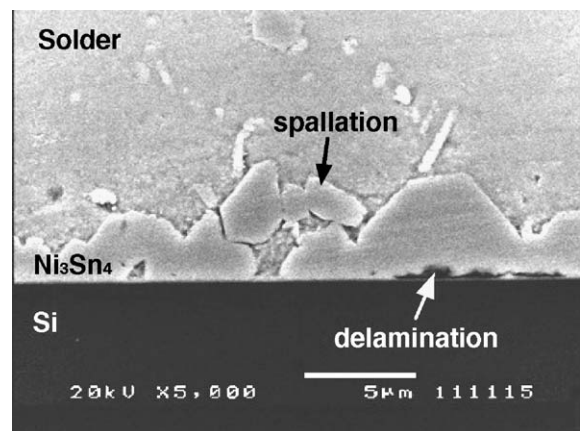


Fig. 8. IMC spallation and delamination from the substrate after being reflowed for 40 min when the sputtered Ni UBM is fully consumed. Arrow indicates the location of delamination.

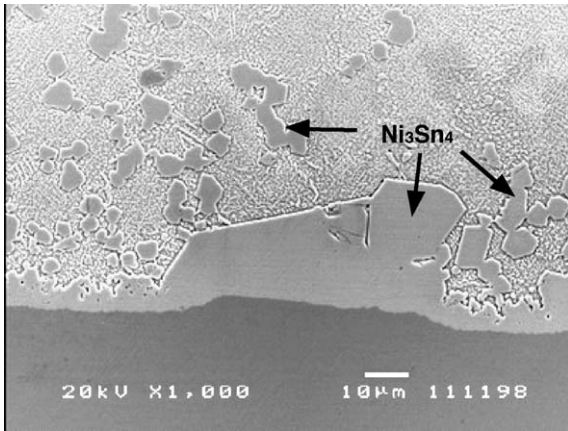


Fig. 9. Observation of IMC spallation and the formation of extremely large  $\text{Ni}_3\text{Sn}_4$  grains. Ni foil (250  $\mu\text{m}$ ) was used as UBM. Samples were reflowed at 251  $^\circ\text{C}$  for 18 h.

grains. Therefore, the tensile stress may not be too serious a concern, especially at the initial stage of reflow. Whether IMC spallation affects the mechanical strength of the solder joint is interesting to investigate, but it is not the objective of this work.

### 3.2. Growth kinetics of the intermetallics

Growth of an IMC layer at liquid–solid interface is a net effect of several interrelated phenomena, such as grain boundary diffusion, volume diffusion through the layer via bulk and grain coarsening. Other factors include IMC spallation and the stresses at the interface, etc. All these are important in determining and controlling the growth kinetics of the IMC layer. In current work, the relationship between reflow time and IMC layer thickness is represented by an empirical power law,

$$\delta = kt^{1/n} \quad (1)$$

where  $\delta$  is the average thickness;  $t$  is the reflow time; and  $k$  and  $n$  are constants. The constants  $k$  and  $n$  are obtained by linear fitting results of log–log plotting from experimental data shown in Fig. 10. The best fits of all experimental data describing the thickening kinetics are listed in Table 1. For the same comparable time frame, IMC growth is faster with Ni–P UBM than with Ni UBM.

The growth kinetics parameter shows that the IMC thickness has an approximate  $t^{1/3}$  dependence on time for both UBMs. This is in agreement with Kim and Tu's [18] work. However, the paradox is that in our work, the IMC grains have formed a continuous layer at long reflow time, which is different from the isolated spherical scallops (with liquid channels in between) as in the case of  $\text{Cu}_6\text{Sn}_5$  IMCs studied by Kim and Tu [18]. As discussed by Ghosh [11], the interpretation of kinetics parameter could be quite complex because the interface process might involve many processes such as grain boundary and/or lattice diffusion,

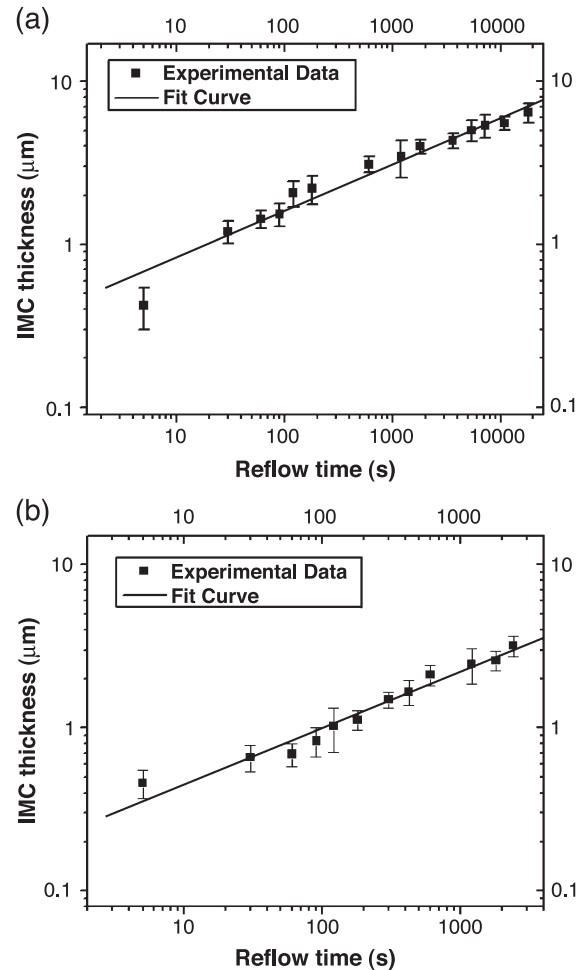


Fig. 10. Log–log plot of  $\text{Ni}_3\text{Sn}_4$  IMC thickening kinetics in two solder/UBM systems during liquid state reaction. (a) Ni–P UBM. (b) Sputtered Ni UBM.

grain grooving, grain coarsening, etc. In other words, the  $t^{1/3}$  growth law may not always be uniquely related to a fixed set of growth mechanisms. As an example, both the liquid-channel scallop model by Kim and Tu [18] and the grain boundary diffusion model by Schaefer et al. [19] predict the same  $t^{1/3}$  growth dependence.

Nevertheless, explanation on the difference in the IMC growth rate between the two UBMs can be attempted from the series of observations made so far. The average thickness of Ni–Sn IMC formed in Ni–P is generally higher than the one formed in pure Ni UBM for the same reflow process. One of the main factors could be the

Table 1  
Kinetics parameters for the growth of  $\text{Ni}_3\text{Sn}_4$  IMC in Sn–3.5Ag/Ni-based UBM systems during liquid state reaction

UBM materials	$k$	$n$	$1/n$
Ni–P alloy	0.43	3.57	0.28
Sputtered Ni	0.20	2.86	0.35

difference between the IMC morphology in these two UBM systems, as revealed by the SEM micrographs in Figs. 3–5. In the case of Ni–P UBM, large intergranular space (grooves) could be seen within the range of the reflow times. These channels allow faster diffusion of Ni across the interface, thereby leading to the formation of a thicker IMC before the dense chunk-type grains cover the whole surface. In the case of Ni UBM, the IMC layer is continuous and relatively densely packed, less space exists in between the grains. The second factor could be the reaction-assisted crystallization of amorphous Ni–P. The crystallization process increases the mobility of Ni by releasing the internal energy through reaction heat. Meanwhile, the columnar structure [12,14] of the formed Ni<sub>3</sub>P layer between Ni<sub>3</sub>Sn<sub>4</sub> and Ni–P UBM provides favorable paths for Ni to diffuse out from the Ni–P layer, resulting in increased growth rate. The third factor is the stress on the IMC layer: compressive stress retards the diffusion while tensile stress promotes diffusion through the layer. All these factors may contribute to the faster IMC growth with Ni–P than with Ni UBM.

### 3.3. Kirkendall void formation in the Ni–P UBM/solder system

On samples of the Sn–3.5Ag/Ni–P UBM system, voids were easily observable under SEM inside the Ni<sub>3</sub>P layer. A typical view of the voids is shown in Fig. 11. Such voids only exist in the samples with the Ni–P UBM after long time reflow (>30 min) and they grow in size with reflow time. No void was observed in the pure Ni system even after reflow at 251 °C for 18 h.

Void formation in the solder/UBM reaction has been reported by other researchers [8,17,20]. The presence of the voids was reported to be either in the Ni<sub>3</sub>Sn<sub>4</sub> phase [17,20] or in the Ni<sub>3</sub>P layer [8]. With the difference in the observed location of void formation comes different explanations for the formation mechanisms. Our observation shows that the

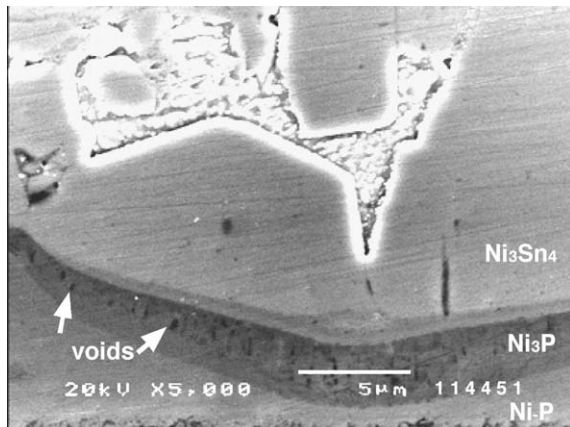


Fig. 11. Kirkendall voids formed in Ni<sub>3</sub>P layer in a Sn–3.5Ag/Ni–P UBM system reflowed at 251 °C for 1 h.

presence of the Ni<sub>3</sub>P layer between the IMC and the Ni–P UBM is a necessary condition for the void formation for this liquid state solder reaction. At the very beginning of the reaction, the formation of Ni<sub>3</sub>Sn<sub>4</sub> depletes Ni from the surface of the electroless nickel alloy, resulting in the crystallization of the P-enriched portion of the alloy to form Ni<sub>3</sub>P. Further supply of nickel for the Ni<sub>3</sub>Sn<sub>4</sub> to grow requires the diffusion of nickel from the unreacted Ni–P through the Ni<sub>3</sub>P layer. Nickel diffusion into the molten solder is much easier, while Sn is prevented from reaching the solid Ni–P UBM layer. This unbalanced elemental diffusion results in the continuous growth of the Ni<sub>3</sub>P layer as well as the nucleation and growth of voids inside the Ni<sub>3</sub>P layer. A detailed discussion was made elsewhere by current authors [21].

The existence of Kirkendall voids in the solder/Ni–P UBM system may have detrimental effect on joint reliability. With increasing reflow time, the voids became an easy path for cracks to go through, resulting in brittle fracture [17,20]. The effect of such voids on the mechanical strength of the solder/UBM systems used in current study will be reported in a future paper.

## 4. Conclusions

Both Ni<sub>3</sub>Sn<sub>4</sub> and Ni<sub>3</sub>P layers form at the Sn–3.5Ag/Ni–P solder joint interface during reflow, while only Ni<sub>3</sub>Sn<sub>4</sub> exists at the interface of the same solder with pure nickel UBM. Needle-type, boomerang-type and chunk-type Ni<sub>3</sub>Sn<sub>4</sub> grains are initially observed during solder/Ni–P reflow reaction. With extended reflow, only chunk-type grains remain. This is the result of the growth and ripening of IMC during liquid state reaction. With the sputtered Ni UBM, only scallop grains with faceted surfaces are present under both short and long reflow durations. Extremely large Ni<sub>3</sub>Sn<sub>4</sub> IMC grains are formed because of the dominant ripening effect at long reflow time. IMC thickness increases with reflow time following a power law with the power indices around 1/3. The IMC growth rate is higher with the Ni–P UBM than with Ni UBM. IMC morphology, crystallization heat and residual stress could be accountable for such a difference. Kirkendall voids are observed inside the Ni<sub>3</sub>P layer in the Ni–P UBM system after long time reflow. Formation of these voids is the result of unbalanced element diffusion of Sn in the solder and Ni in the UBM. Such a mechanism does not exist in pure Ni UBM—therefore, no voids are formed there.

## Acknowledgements

This work was supported by an Academic Research Fund from the Nanyang Technological University. Helpful discussion with Prof. Andriy Gusak of the Cherkasy National University, Ukraine, is gratefully acknowledged.

## References

- [1] A.Z. Miric, A. Grusd, *Soldering & Surface Mount Technology* 10 (1998) 19.
- [2] B. Trumble, *IEEE Spectrum*, vol. 5, Institute of Electrical and Electronics Engineers, USA, 1992, p. 55.
- [3] E. Jung, R. Aschenbrenner, C. Kallmayer, P. Coskina, H. Reichl, *International Symposium on Advanced Packaging Materials*, Georgia, U.S.A., March 11–14, 2001, International Microelectronics and Packaging Society, Washington, USA, 2001, p. 119.
- [4] E.P. Wood, K.L. Nimmo, *Journal of Electronic Materials* 23 (1994) 709.
- [5] N.C. Lee, *Soldering & Surface Mount Technology* 9 (1997) 65.
- [6] K.N. Tu, K. Zeng, *Materials Science and Engineering R34* (2001) 1.
- [7] H.K. Kim, K.N. Tu, P.A. Totta, *Applied Physics Letters* 68 (1996) 2204.
- [8] K. Zeng, K.N. Tu, *Materials Science and Engineering R38* (2002) 55.
- [9] R.J.K. Wassink, *Soldering in Electronics*, Electrochemical Publications, IOM, 1984.
- [10] P.G. Kim, J.W. Jang, T.Y. Lee, K.N. Tu, *Journal of Applied Physics* 86 (1999) 6746.
- [11] G. Ghosh, *Journal of Applied Physics* 88 (2000) 6887.
- [12] P.L. Liu, J.K. Shang, *Metallurgical and Materials Transactions. A, Physical Metallurgy and Materials Science* 31A (2000) 2857.
- [13] K.C. Hung, Y.C. Chan, C.W. Tang, H.C. Ong, *Journal of Materials Research* 15 (2000) 2534.
- [14] J.W. Jang, P.G. Kim, K.N. Tu, *Journal of Applied Physics* 85 (1999) 8456.
- [15] K.L. Lin, Y.C. Liu, *IEEE Transactions on Advanced Packaging* 22 (1999) 568.
- [16] C.E. Ho, W.T. Chen, C.R. Kao, *Journal of Electronic Materials* 30 (2001) 379.
- [17] Y.D. Jeon, K.W. Paik, K.S. Bok, W.S. Choi, C.L. Cho, *Journal of Electronic Materials* 31 (2002) 520.
- [18] H.K. Kim, K.N. Tu, *Physical Review B* 53 (1996) 16027.
- [19] M. Schaefer, R.A. Fournelle, J. Liang, *Journal of Electronic Materials* 27 (1998) 1167.
- [20] Y.D. Jeon, K.W. Paik, K.S. Bok, W.S. Choi, C.L. Cho, *Electronic Components and Technology Conference*, San Diego, U.S.A., May 29–June 1, 2001, *IEEE Proceeding*, vol. 51 (2001), p. 1326.
- [21] M He, Z. Chen, G. Qi, *Acta Materialia* 52 (2004) 2047.